14th European Signal Processing Conference (EUSIPCO 2006), Florence, Italy, September 4-8, 2006, copyright by EURASIP

SEGMENTATION OF REMODELLING REGIONS IN BONE MICRO-CT IMAGES : INFLUENCE OF DENOISING

Zsolt Peter, Sabine Rolland du Roscoat, Françoise Peyrin

CREATIS, UMR CNRS 5515 ; Inserm U630 ; INSA, Bâtiment Blaise Pascal
7, avenue Jean Capelle, 69621 Villeurbanne Cedex, France
ESRF – BP 220 - 38043 Grenoble, France
phone: +(33) 4 38 88 19 63 , fax: +(33) 4 76 88 22 52, email: zpeter@esrf.fr

ABSTRACT

Synchrotron radiation 3D micro-CT providing quantitative images of bone samples opens new perspectives for assessing bone metabolism. The purpose of this paper is to evaluate the possibility of segmenting remodeling regions from such images acquired at a spatial resolution of 10 µm. Segmenting remodeling regions within the bone phase is not an easy task. Although remodeling regions can be visually distinguished, their contrast with respect to bone may be very weak and close to the standard deviation of noise. We propose a segmentation scheme based on a customized region growing associated to a denoising process. We consider denoising methods based on wavelets and anisotropic diffusion. Our results show that a corrupted image can be well restored, essentially without compromising image resolution. Thus the segmentation of correct remodeling zones in the bone is more realistic on the denoised images.

1. INTRODUCTION

Osteoporosis is a bone fragility disease based on reduced bone mass and alterations of bone-micro-architecture. Bone micro-architecture is increasingly investigated by micro-tomography (CT) techniques, which as compared to histology, is a non destructive technique and may provide three-dimensional information [1]. A number of micro-CT systems are now commercialized and provide images at spatial resolution up to a few micrometers. After segmenting bone from background, three-dimensional quantitative parameters of bone micro-structure are typically calculated. However densitometric information within bone phase is generally not available due to beam hardening and limited signal to noise ratio when using standard x-ray sources. Coupling micro-CT to synchrotron sources allow to overcome these limitations and provide quantitative images [2].

In previous works, we showed that synchrotron micro-CT enables to recover the mineral concentration in bone tissue, also called the degree of mineralization of bone (DMB). The accuracy of the system was evaluated by using solutions mimicking hydroxyapatite, the main component of bone, at different known concentrations [3]. The method was applied to analyze the effect of a treatment of osteoporosis: while there were no significant differences in micro-architecture parameters, the DMB tended to increase after treatment [4].

The quantification of the DMB provides important information about the metabolism of bone. Indeed bone is constantly remodeled, which means that it is sequentially resorbed and reconstructed. After reconstruction, its mineral concentration in localized regions increases progressively.

Figure 1 illustrates a 2D slice in a cortical bone sample acquired using synchrotron micro-CT system developed at ESRF (European Synchrotron Radiation Facility, Grenoble, France). The slice is a 660x360 image with a voxel size of 10 µm. Remodeling regions, characterized by a darker gray level traducing a smaller mineral concentration, and thus more recent bone, may be observed around some pores [5].

Till now, the quantification of DMB has been based on global parameters, such as the mean and standard deviation calculated on the entire bone phase. The purpose of this paper is to evaluate the possibility of identifying the different remodeling regions which would allow getting new characteristics about bone metabolism.

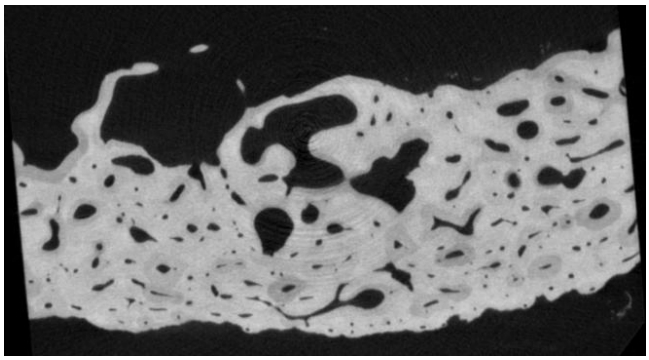

Figure 1 - Original cortical bone slice image

The problem is the segmentation of remodeling regions. If the segmentation of bone from background is straightforward, segmenting remodeling regions within the bone phase is not an easy task. Although theses regions can be visually perceived, their contrast with respect to bone may be very weak and close to the standard deviation of noise. In addition, ring artifacts related to image formation may also corrupt image quality. Removing or at least significantly reducing noise and artifacts will be important in view to perform quantitative analysis. However, note that since the structure of interest is small, the resolution of the image must be preserved.

In this paper, we propose a segmentation scheme based on a customized region growing associated to a denoising process. We consider denoising methods based on wavelets and compare the results to anisotropic diffusion. The comparison is performed on a synthetic image. Finally the method is applied to a cortical bone image. Our results show that a corrupted image can be well restored, essentially without compromising image resolution, and that this step is essential for segmentation.

2. SEGMENTATION SCHEME

2.1 Position of the problem

Figure 2 shows the histogram of image in Figure 1. The histogram is clearly bimodal, the first peaks corresponding to background and pores, the second peak, to the entire bone phase. The later does not exhibiting a multimodal distribution, simple thresholding is clearly insufficient for our problem.

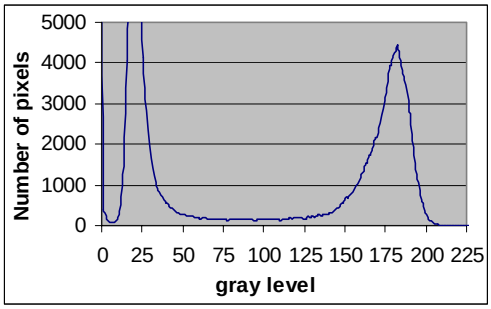

Figure 2 - Original cortical bone slice image

In addition, the statistical analysis of the image shows that the standard deviation of noise is around 7 (gray level), and is of the same order of magnitude that the contrast between some remodeling regions and bone surroundings. Thus contour based approaches are not efficient.

2.2 Region growing process

Among the different possible approaches to image segmentation, we propose to use a customized region growing taking into account biological prior information. According to bone physiology, remodeling regions are located around pores and are relatively elliptic although their shapes may vary. The method proceeds as follows.

First, the bone phase is segmented from background by simple thresholding. The contours are detected by a simple gradient method and the exterior contour is eliminated. The pore contours are then obtained and tracked to get closed and 1 pixel-thick contours. Then a connected component analysis is performed in order to label each pore contour. This image is then used to initialize the region growing process.

The region growing process is then performed by using a homogeneity criterion on the region. The number of connected pore sets the number of regions in the image. For each region, labeled by l, a neighbor pixel $\mathbf{x}$ is labeled in the region if :

$$|f(\mathbf{x}) - m(l)| < \alpha\sigma(l) \qquad (1)$$

where $f(\mathbf{x})$ is the image gray level, $m(l)$ and $\sigma(l)$ are the current mean and standard deviation of the region, and α is a parameter.

However the direct application of the algorithm to the image give poor results, denoising schemes prior to segmentation are considered.

3. DENOISING PROCESS

3.1 Wavelet Based Denoising

Wavelet based denoising has been showed efficient in some applications [6]. Basically, the noisy image is transformed into the wavelet domain, then the wavelet coefficients are subjected to soft or hard thresholding, and in the last step the result is inverse-transformed. If W denote the wavelet transform (and w the set of the wavelet coefficients), then the whole denoising process with a threshold t, amounts to a non-linear operator T_η :

$$T_\eta = W^{-1} \circ \eta_t \circ W \qquad (2)$$

where $\eta_t(w) = sgn(w)(|w| - t)_+$ for the soft thresholding, and $\eta_t(w) = w\ 1_{\{|w|>t\}}$ for the hard thresholding.

The application of this method yields some oscillations which are especially pronounced in the vicinity of discontinuities and rapid changes [7]. These are "pseudo-Gibbs" oscillations caused by the fact that we have used only a subset of the full set of basis elements. In contrast to the classical Gibbs-phenomena associated with Fourier analysis, the "pseudo-Gibbs-phenomena" are much better behaved, much better localized and much more moderate in oscillation; nevertheless they could influence a correct segmentation of the cortical bone image.

3.2 Translation-Invariant (TI) Denoising

These artifacts exhibited by denoising with traditional (orthogonal, maximally-decimated) wavelet transforms are due to the lack of translation invariance of the wavelet basis. The main idea of the "second generation denoising" method, proposed in [7], is the following: for a range of shifts, one shifts the data, denoises the shifted data and then unshifts the denoised data. Doing this for each of a range of shifts, and averaging the several results so obtained, produces a reconstruction subject to far weaker Gibbs phenomena.

For a signal $(x_t : 0 \le t < n)$, let S_h denote the circulant shift by $h \in N$, $(S_h x)_t = x_{(t+h) mod\, n}$. This operator is unitary, and hence invertible: $S_{-h} = (S_h)^{-1}$. In term of operators, the idea of shifting to avoid artifacts is the following: given an analysis technique T, calculate the shifted version $\tilde{T}$, for a range H of shifts (all n for instance) and average over the several results so obtained:

$$\tilde{T}(x; (S_h)_{h\in H}) = Aver_{h\in H} S_{-h}(T(S_h(x))). \qquad (3)$$

Cycle-spinning over the range of all circulant shifts can be accomplished in order $n log_2(n)$ time; it is equivalent to

denoising using the undecimated or stationary wavelet transform.

In the following, our analysis technique T is a non-linear operator T_η, where $T_\eta = W^{-1} \circ \eta_t \circ W$ and η_t is the hard thresholding with a threshold t. Hard thresholding and translation invariance combined give both good visual characteristics and good quantitative characteristics [7]. As mentioned by Coifman and Donoho, when used with the right wavelets, thresholding the non-decimating transform is mathematically equivalent to cycle-spinning with all n circulant shifts.

3.3 Anisotropic Diffusion

The anisotropic diffusion is a popular filtering process aiming to eliminate the noise from an image [8]. This method is based on the physical principles of the diffusion between fluids: the equation of diffusion is similar to that of the local concentrations of a fluid which equilibrates without matter creation or destruction. In order to perform anisotropic diffusion of an image we will follow the classical Perona and Malik's algorithm [9]. This process smoothes regions while preserving, and enhancing, the contrast at sharp intensity gradients like contours.

Consider the anisotropic diffusion equation:

$$\frac{\partial f}{\partial t} = div(c(\mathbf{x},t)\nabla f) = c(\mathbf{x},t)\Delta f + \nabla c \cdot \nabla f \qquad (4)$$

where div indicates the divergence operator and ∇ and Δ respectively the gradient and Laplacian operators, with respect to the spatial variables $(\mathbf{x})$. Here $f(\mathbf{x},t)$ represents a family of images with the initial condition $f(\mathbf{x},0) = f(\mathbf{x})$ being the original image. It was shown that a diffusion in which the conduction coefficient $c = c(\mathbf{x},t)$ is chosen locally as a function of the magnitude of the gradient of the brightness function, *i.e.*,

$$c(\mathbf{x},t) = g\left(\left\|\nabla f(\mathbf{x},t)\right\|\right) \qquad (5)$$

will not only preserve, but also sharpen, the brightness edges if the function g is chosen properly. Different functions were used for g giving perceptually similar results [10]. The test images for this paper were obtained using

$$g\left(\left\|\nabla f\right\|\right) = \frac{1}{1 + \left(\frac{\left\|\nabla f\right\|}{K}\right)^2} \qquad (6)$$

which favors wide regions over smaller ones. If the edge threshold parameter K is low, small intensity gradients are able to block conduction and hence diffusion across step edges. A large value reduces the influence of intensity gradients on conduction.

4. RESULTS

4.1 Synthetic phantom

We first simulated a 512x512 synthetic image presenting some characteristics of the physical bone images. The phantom was made of five ellipses embedded in a white surrounding (gray level=249) with the following gray levels: 132, 200, 235, 239 and 244. The number of pixels in each region is indicated in the first line of Table 1. The image was corrupted with gaussian noise with a standard deviation of 7. The noisy image is shown in Figure 3 (noise is not too apparent due to size reduction). In the histogram of the image (not shown), the peaks of the highest gray level ellipses overlap with that of the surrounding.

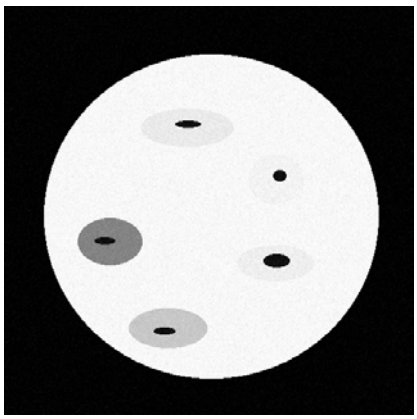

Figure 3 – Noisy synthetic image

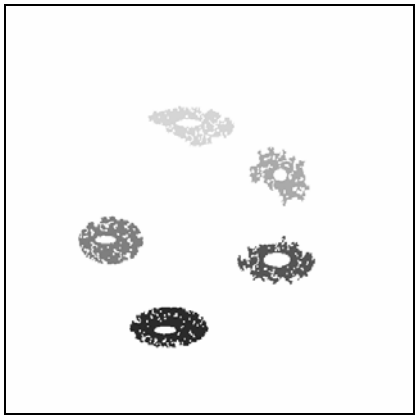

Figure 4 – Segmentation applied to the noisy synthetic image.

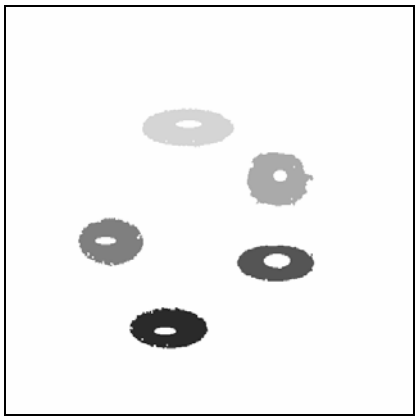

Figure 5 – Segmentation applied to the noisy synthetic image after denoising by the translation-invariant wavelet method.

The results of the region growing segmentation on the noisy synthetic image are presented on Figure 4. The algorithm delivers an image where each region has a different label, displayed in gray levels. The relative error between the estimated and theoretical number of pixels in each region is presented in the second line of Table 1. There is a clear underestimation of each region. Trying to incorporate morphology operations (closing) during the segmentation process yields little improvement and perturb the homogeneity criterion.

The three denoising methods were then applied before segmentation: soft-thresholding wavelets (Wav), translation-invariant wavelets (TI-wav) and anisotropic diffusion (Diff). Both wavelet transforms used Daubechies4 wavelet [11]. The segmentation process is neatly improved. The quantitative errors in each region with the different methods are summarized in Table 1. The first line indicates the exact values. The second line shows the results obtained from the noisy image without denoising, and the three last lines corresponds to the results obtained applying the denoising process before region growing. The results show that denoising clearly improves the segmentation process. The translation-invariant wavelet method and anisotropic diffusion give close results. The relative error summed on the four more difficult regions (gray level >= 200), is equal to -0,9% with the translation-invariant wavelet method and -5,1% with the anisotropic diffusion method. The results obtained with the translation-invariant wavelet method giving the best performances are illustrated on Figure 5.

Gray level	132	200	235	239	244
Original	3565	3653	4148	2959	3280
Noisy	-38,6%	-34,0%	-52,0%	-34,9%	-48,2%
Wav	-36,4%	-39,4%	-21,5%	-14,0%	-4,9%
TI-Wav	-8,8%	-7,1%	-7,3%	-3,8%	16,7%
Diff	-5,4%	-13,7%	-7,4%	-1,0%	3,8%

Table 1 : Results of segmentation. First line: number of pixels in each region with the given gray level. Next lines: relative error between the estimated and exact number of pixels for each method, in each region.

4.2 Bone images

The same process was applied to the physical bone image. We present the application of the method to the rough image (Figure 7) as well as to the denoised image using the translation-invariant wavelet method (Figure 8). On Figure 6 we have represented the structures (containing also parts of the ring artifacts) which were removed by the denoising. The zones detected in the denoised image are more compact with more regular contours. The segmented original image has the typical noise corrupted behavior. These figures show the effective improvement in the quality of segmentation by using a denoising based pre-treatment on the image. Finally, on Figure 9 we can check the localization and the shape of detected remodeling zones, superimposed to the original image. Although some remodeling zones are missing, a majority of them are detected at the good location.

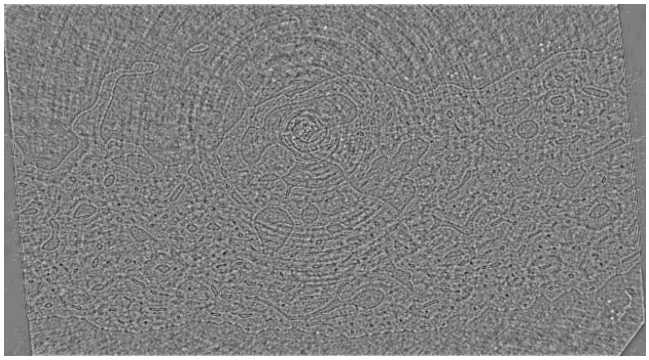

Figure 6 – The removed noise with TI wavelet denoising

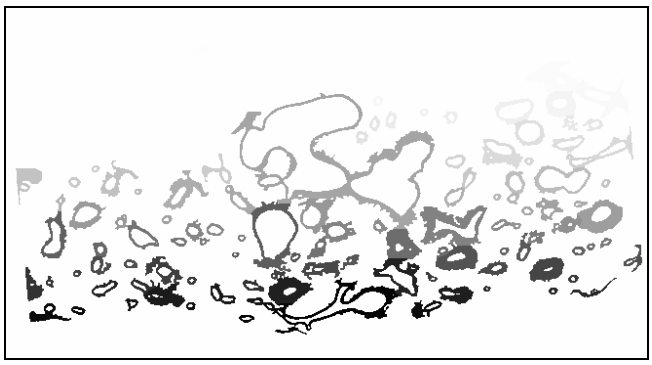

Figure 7 – Segmentation applied to the bone image.

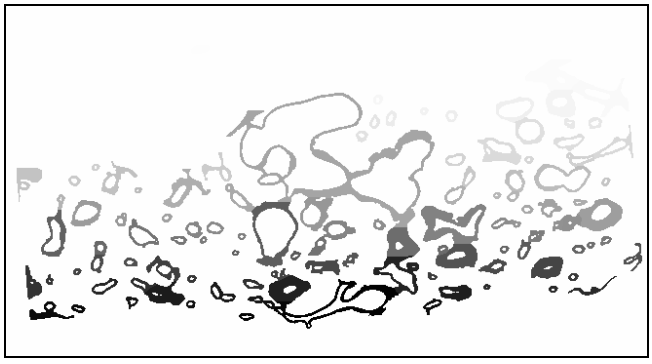

Figure 8 – Segmentation applied to the bone image after denoising by the translation-invariant wavelet method.

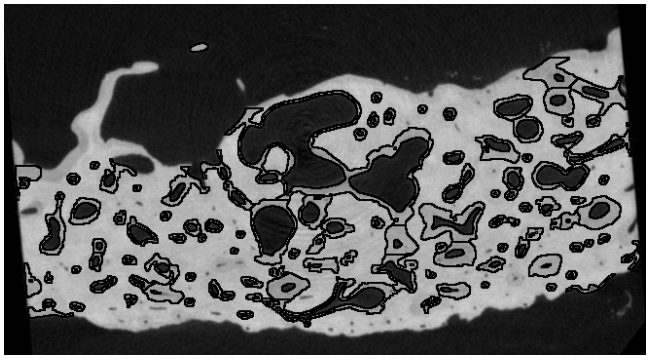

Figure 9 – Localization of segmented zones: superposition of the contours detected after segmentation to the original image.

5. DISCUSSION AND PERSPECTIVES

The method presented in this paper for segmenting remodeling regions in high resolution micro-CT images is encouraging. Segmenting remodeling zones in 3D has yet never been performed.

We used a relatively simple segmentation method based on region growing. However this method gave us the opportunity to use the prior biological knowledge that the remodeling regions are searched around pores. Other approaches such as K-means or a region growing method using the energy model of Mumford and Shah [12] were tested. The later is based on the minimization of an energy term incorporating a constraint on the curvature. Although this method seemed attractive, the results showed over-segmentations: false detections appeared in bone background and a remodeling zone corresponding to a physiological entity could be split in many sub-regions.

An efficient denoising method preserving the spatial resolution in the images has proven to be mandatory prior to segmentation. In this respect, the translation-invariant wavelet method provided high quality result. Perspectives could be to use complex wavelet transform which were more recently introduced and offer advantages in terms of localization.

Our final goal is to extend the method to 3D images. The pores, as may be seen in 3D, are cylindrical structures with a main axis roughly perpendicular to the direction of the slice [5]. Thus a 2D slice by slice approach is acceptable in a first step. However the extension of the method in 3D could improve the robustness of the segmentation.

ACKNOWLEDGEMENT

We thank Valérie Bousson, Catherine Bergot and Pr. Jean Denis Larédo from Hospital Lariboisière, Paris, for providing the bone samples and for data acquisition.

REFERENCES

[1] R. Muller, T. Hildebrand, R. Ruegsegger, “Non-invasive bone biopsy: a new method to analyse and display the three-dimensional structure of trabecular bone”, Phys. Med. Biol. 1994 Jan; 39(1):145-64.

[2] M. Salome, F. Peyrin, P. Cloetens, C. Odet, A.M. Laval-Jeantet., J Baruchel, P Spanne, “A synchrotron radiation microtomography system for the analysis of trabecular bone samples”, *Med. Phys.*, 1999, 26(10) : 2194-2204

[3] S. Nuzzo, F. Peyrin, E. Martín-Badosa, M.H. Lafage-Proust, G. Boivin, “Assessment of Bone Mineral Content from 3D Synchrotron Radiation Microtomography Images”, *IEEE Transactions On Nuclear Science*, June 2001, Vol. 48, n° 3 (Pt 2), p. 859 –863.

[4] S. Nuzzo, F. Peyrin, E. Martin-Badosa, M.H. Lafage-Proust, G. Boivin, “Quantitative analysis of mineral bone variation in 3D Synchrotron Radiation Microtomography images”, *Journal of Bone and Mineral Research* 2003, 18(4) : 760-768.

[5] V. Bouson, F. Peyrin, C. Bergot, M. Hausard, A. Sautet, J.D. Larédo, “Cortical bone of the human femoral neck : three-dimensional appearance and porosity using synchrotron radiation”, *Journal of Bone and Mineral Research* 2004, 19(5) : 794-801

[6] S. Mallat, A Wavelet Tour of Signal Processing, Academic Press, San Diego, CA, 1997.

[7] D. Donoho, R.R. Coifman, “Translation Invariant De-Noising”, Wavelets and Statistics, A. Antoniadis and G. Oppenheim, Eds. New York: Springer-Verlag, 1995, pp. 125--150.

[8] P.D. Kovesi, *MATLAB and Octave Functions for Computer Vision and Image Processing*, School of Computer Science & Software Engineering, University of Western Australia.: http://www.csse.uwa.edu.au/~pk/research/matlabfns/

[9] P. Perona, J. Malik, “Scale space and edge detection using anisotropic diffusion”, *IEEE Trans. Pattern Anal. Mach. Intell.*, vol. 12, no. 7, pp. 629--639, Jul. 1990.

[10] G. Gilboa, N. Sochen, Y. Y. Zeevi, “Complex Diffusion Processes for Image Filtering”, *Scale-Space 2001, LNCS 2106*, pp. 299-307, Springer-Verlag 2001.

[11] D. Donoho, Wavelab 802 software, http://www-stat.stanford.edu/~wavelab

[12] F. Dibos, G. Koepfler, “Global total variation minimization”, *SIAM Journal on Numerical Analysis*, no. 37, pp. 646-664, 2000.